

# Is dark matter present in NGC 4736? An iterative spectral method for finding mass distribution in spiral galaxies

Joanna Jałocha, Łukasz Bratek, Marek Kutschera<sup>1</sup>

*The Henryk Niewodniczański Institute of Nuclear Physics, Polish Academy of Science,  
Radzikowskiego 152, 31-342 Kraków, Poland*

## ABSTRACT

An iterative method for reconstructing mass distribution in spiral galaxies using a thin disk approximation is developed. As an example, the method is applied to galaxy NGC 4736; its rotation curve does not allow one to employ a model with a massive spherical halo. We find a global mass distribution in this galaxy (without non-baryonic dark matter) that agrees perfectly with the high resolution rotation curve of the galaxy. This mass distribution is consistent with the *I*-band luminosity profile with the mean mass-to-light ratio  $M/L_I = 1.2$ , and also agrees with the amount of hydrogen observed in the outermost regions of the galaxy. We predict the total mass of the galaxy to be only  $3.43 \times 10^{10} M_\odot$ . It is very close to the value predicted by the modified gravity models and much less than the currently accepted value of  $5.0 \times 10^{10} M_\odot$  (with  $\approx 70\%$  of the mass in a dark matter halo).

*Subject headings:*

### 1. Introduction

Determination of dynamical masses of spiral galaxies is a decisive step in establishing empirically the clustering scale of dark matter. The Cold Dark Matter model predicts a hierarchy of scales, from a dwarf sub-halo scale of  $10^6$  of solar masses up to a galaxy cluster size. There is a strong evidence from the *X*-ray observations of galaxy clusters, and from detecting dark matter with gravitational lensing [Massey et al. 2007] for a 1 Mpc scale, which is the galaxy cluster scale. At the galactic size scale (of the order of 10 – 50 kpc), there are contradictory results. Dark matter was not observed in some elliptical galaxies [Romanowsky et al. 2003]. As for the spiral galaxies, it was pointed out that the amount of dark matter in the disk of the Milky Way galaxy near the Sun is insignificant [Kuijken & Gilmore 1989]. Moreover, mass estimates of spiral galaxies are model-dependent [Sofue & Rubin 2001].

In the following we propose an Iterative Spectral Method to reconstruct mass distribution in the spiral galaxies. The method is based on the thin disk model [Toomre 1963, Nordsieck 1973] which offers the possibility to obtain mass density distribution from the observed rotation curve [Binney & Tremaine 1987]. With the Iterative Spectral Method this reconstruction is unique, provided there is observational data about the hydrogen density in the regions outside of rotation velocity measurements. Without such data one can also extrapolate hydrogen measurements by assuming its falloff profile that would be physically acceptable. One should also take into account the abundance of helium which is proportional to that of hydrogen. In this way we obtain a complete set of data in the complementary regions of a given galaxy. Complete

data are required to eliminate cutoff errors that normally result from cutting-off integration in an integral that relates rotational velocity to disk surface mass density at the radius where measurements of a rotation curve end. We shall call the radius the 'cutoff radius' and denote it by  $R$ .

In fact, in early days of galactic research the thin disk model was applied to infer the galactic masses from the measured rotation curves. However, large errors of measurements of rotational velocities practically made the surface mass density reconstruction impossible [Binney & Tremaine 1987]. To avoid uncertainties in the thin disk mass reconstruction it became customary to a priori divide spiral galaxies into three major components: bulge, disk and spherical halo. Then a several parameter fit was made determining the properties of those components. Although this approach is physically appealing, the amount of arbitrariness in such a division is unacceptable. In particular, the most massive component of this construction - the spherical halo - stands on the weakest empirical footing.

In this paper we address the problem of determination of masses of spiral galaxies with rotation curves violating the sphericity condition at large radii. One expects that the disk model should approximate mass distribution in such galaxies better than models assuming a massive spherical halo. The reconstructed surface mass density found for galaxy NGC 4736 approaches the hydrogen density at the outskirts of the galaxy, the rotation curve is perfectly matched in the measured range, and its continuation is predicted further out into the Keplerian regime. Thus the disk model performs much better in this case than models including the spherical dark halo.

To see why the assumption of the existence of spherical halo seems to be unjustified for a class of spiral galaxies, we consider as an example the galaxy NGC 4736. It was

<sup>1</sup>Jagellonian University, Institute of Physics, Reymonta 4, 30-059 Kraków, Poland.

found (Kent [1987]) that most of the mass (68%) in this galaxy is concentrated in a spherical dark halo, mainly at larger radii. At these distances surfaces of constant gravitational potential are almost spherical. Therefore one would expect in this region the rotation curve predicted by the Kent's analysis to satisfy the sphericity condition. For a spherically symmetric mass distribution the Keplerian mass function,  $M_K(\rho) \equiv G^{-1} v^2(\rho)\rho$ , corresponding to rotational velocity  $v(\rho)$ , should be a nondecreasing function of the radial distance from the center  $\rho$ , that is,

$$v^2(\rho_1)\rho_1 \leq v^2(\rho_2)\rho_2, \quad \text{if only} \quad \rho_1 \leq \rho_2.$$

The experimental rotation curve of NGC 4736 violates this condition for  $\rho \gtrsim 6$  kpc, see figure 1, whereas the best-fitting solution for the rotation curve found by Kent satisfies this condition. At large radii the best-fitting rotational velocity is also greater from the observed by a factor of  $\approx 1.2$ . The total mass should be therefore  $\approx 5.9 \times 10^{10} M_\odot / (1.2)^2 = 4.1 \times 10^{10} M_\odot$  rather than  $5.9 \times 10^{10} M_\odot$  as found in [Kent 1987] (at the currently accepted distance 5.1 Mpc to NGC 4736 the mass is even less,  $\approx 3.5 \times 10^{10} M_\odot$ ). This shows that the mass distri-

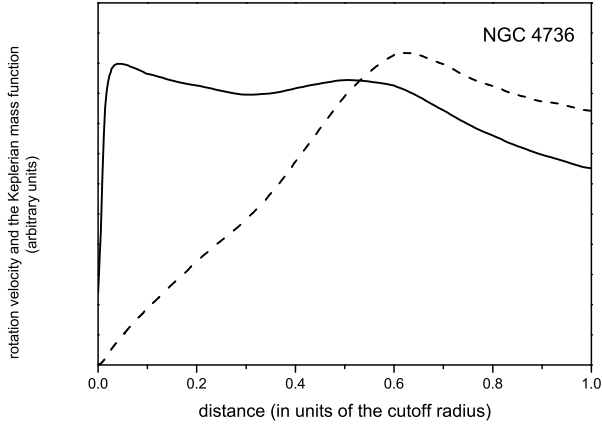


Fig. 1.— Negative sphericity test for spiral galaxy NGC 4736. The figure shows experimental rotation curve (solid line) and the corresponding Keplerian mass function defined by  $M_K(\rho) = G^{-1} \rho v^2(\rho)$  (dashed line). The Keplerian mass function is not increasing at all distances, therefore a massive spherical halo in the approximation of circular orbits is excluded and should be replaced with an extended flattened component.

bution in the galaxy cannot be dominated by a spherical component and that it would be more appropriate to assume more extended disk components in similar galaxies in place of massive spherical halos.

The global disk model has been used recently [Takamiya & Sofue 2000], however the procedure of cutting-off integrals applied therein lead to overestimation of surface density at larger radii for galaxies with declining rotation curves. For example, surface density in the galaxy NGC 4736 could be reliably determined only within a radius of less than 6 kpc. But the experimental data available for this galaxy enable one to find a much better determination of mass distribution as far as 16 kpc from the center. An improved

approach was presented in [Kostov 2006], where rotation curves were assumed Keplerian in the unobserved regions. This procedure is still unsatisfactory, as velocities of test particles on circular orbits encircling a disk-like object need not be Keplerian. Besides no comparison with the observed mass density has been done.

## 2. Iterative Spectral Method

Let  $v_R = v(R)$  denote the last measured value of rotational velocity at cutoff radius  $R$ . We define also a dimensionless function  $u(x) = v(xR)/v_R$  for describing rotation curve, where  $x = \rho/R$  measures distances in units of the cutoff radius (we work in cylindrical coordinates  $(\rho, \phi, z)$ ).

Below we shall derive equations that are fundamental for the iteration method we present later on.

### 2.1. Basic equations of disk model

Let the  $z = 0$  plane represent the galactic disc. It is assumed that most of galactic mass is concentrated in its vicinity. A  $z$ -symmetric and cylindrically symmetric vacuum gravitational potential is given by

$$\Phi(\rho, z) = -2\pi v_R^2 \int_0^\infty \hat{\sigma}(\omega) J_0\left(\omega \frac{\rho}{R}\right) e^{-\omega \frac{|z|}{R}} d\omega.$$

A discontinuity of  $\frac{1}{2\pi G} \vec{\nabla} \Phi$  in the direction normal to the  $z = 0$  plane is interpreted as a surface mass density  $\sigma(\rho)$  of the galactic disk

$$\sigma(\rho) = \frac{v_R^2}{GR} \int_0^\infty \omega \hat{\sigma}(\omega) J_0\left(\omega \frac{\rho}{R}\right) d\omega, \quad (2-1)$$

thus  $\hat{\sigma}(\omega)$  is the Fourier-Bessel transform of  $\sigma(\rho)$

$$\hat{\sigma}(\omega) = \frac{GR}{v_R^2} \int_0^\infty x \sigma(Rx) J_0(\omega x) dx. \quad (2-2)$$

Modelling of galactic rotation curves usually assumes that orbits of stars are circular and concentric, then  $v^2(\rho)|_{z=0} = \rho \partial_\rho \Phi(\rho, 0)$ , therefore,

$$u^2(x) = 2\pi x \int_0^\infty \omega \hat{\sigma}(\omega) J_1(\omega x) d\omega. \quad (2-3)$$

By substituting (2-2) to (2-3) one can show that<sup>1</sup>

$$v^2(\rho) = 4G\rho \cdot \mathcal{P} \left( \int_0^\rho \sigma(\chi) \frac{\chi E\left(\frac{\chi}{\rho}\right)}{\rho^2 - \chi^2} d\chi \right)$$

<sup>1</sup>We used the following identities [Ryzhik & Gradshteyn 1951]:  $\omega^{-1} \partial_x (x J_1(\omega x)) = x J_0(\omega x)$  and

$$\int_0^\infty d\omega J_1(\omega \xi) J_1(\omega x) = \frac{2}{\pi} \begin{cases} [K(\xi/x) - E(\xi/x)] \xi^{-1}, & 0 < \xi < x, \\ [K(x/\xi) - E(x/\xi)] x^{-1}, & 0 < x < \xi, \end{cases}$$

where the complete elliptic functions are defined by

$$K(\kappa) = \int_0^{\pi/2} \frac{d\phi}{\sqrt{1 - \kappa^2 \sin^2 \phi}}, \quad E(\kappa) = \int_0^{\pi/2} d\phi \sqrt{1 - \kappa^2 \sin^2 \phi}.$$

$$- \int_{\rho}^{\infty} \sigma(\chi) \left[ \frac{\chi^2 E\left(\frac{\rho}{\chi}\right)}{\rho(\chi^2 - \rho^2)} - \frac{K\left(\frac{\rho}{\chi}\right)}{\rho} \right] d\chi, \quad (2-4)$$

where  $\mathcal{P}$  stands for the "principal value integral". The simple pole  $\chi = \rho$  dominates the logarithmic divergence in  $K(\rho/\chi)$ , thus the principal value integral is easily tractable numerically and can be calculated with high accuracy. The inverse of the above integral reads<sup>2</sup>

$$\sigma(\rho) = \frac{1}{\pi^2 G} \mathcal{P} \left( \int_{\rho}^{\infty} v^2(\chi) \frac{E\left(\frac{\rho}{\chi}\right)}{\chi^2 - \rho^2} d\chi + \int_0^{\rho} v^2(\chi) \left[ \frac{K\left(\frac{\chi}{\rho}\right)}{\rho \chi} - \frac{\rho}{\chi} \frac{E\left(\frac{\chi}{\rho}\right)}{\rho^2 - \chi^2} \right] d\chi \right), \quad (2-5)$$

Unfortunately, this nice formula is not very useful for determining  $\sigma(\rho)$  directly from  $v(\rho)$ , as the observed rotation curves have naturally a cut-off, and therefore the integration cannot be carried out.<sup>3</sup> For example, the closer  $\rho$  is to cutoff radius  $R$ , the more  $\sigma(\rho)$  is underestimated by cutting off the integration at  $R$ . In order to overcome this unpleasant feature of disk geometry one may use another, complementary set of the experimental data concerning mass distribution at  $\rho > R$ . A global mass density and the corresponding global rotation curve can be found iteratively that would both satisfy the relations (2-4) and (2-5) and be consistent with the observations.

## 2.2. A series approximation of the surface density

Below we shall find a first approximation to  $\sigma(\rho)$  directly from the observed part of rotation curve.

A function  $u^2(x)/x$  defined on the unit interval  $x \in (0, 1)$ , can be expressed in terms of a series of independent functions. In particular, if  $u^2(x)/\sqrt{x}$  is integrable over the interval, a complete set of orthogonal functions on  $x \in (0, 1)$  can be constructed from the Bessel function  $J_1$  [Lebediev 1953]. Then

$$\frac{u^2(x)}{x} = \sum_k \hat{\sigma}_k J_1(\omega_k x), \quad 0 < x < 1, \quad J_0(\omega_k) = 0, \quad \omega_k > 0. \quad (2-6)$$

The summation is taken over all consecutive zeros  $\omega_k > 0$  of the Bessel function  $J_0$ . By multiplying both sides by  $x J_1(\omega_m x)$  and integrating over  $x \in (0, 1)$ , we find that

$$\hat{\sigma}_k = \frac{\omega_k}{J_1(\omega_k)} \mu_k, \quad \mu_k = \frac{2}{\omega_k} \int_0^1 u^2(x) \frac{J_1(\omega_k x)}{J_1(\omega_k)} dx. \quad (2-7)$$

The amount of information encoded in the enumerable sequence  $\hat{\sigma}_k$  is insufficient for determining the transform  $\hat{\sigma}(\omega)$  which is a continuum of numbers. Therefore,  $\sigma(\rho)$

cannot be determined accurately from the observed rotation curve alone, even in the region  $\rho < R$ . However, the elements of the sequence can be still linearly combined to approximate  $\hat{\sigma}(\omega)$ . Note, that every such approximation is equivalent to choosing a particular extrapolation of a rotation curve beyond its cutoff radius.

There are some mathematical subtleties regarding this extrapolation. Let us assume first that we put  $v(\rho) = 0$  for  $\rho > R$  and  $v(\rho) = v_R/2$  at a single point  $\rho = R$ . Then we can use the representation (2-6) for  $x < 1$ , and for  $x > 1$  we set  $u = 0$ . From the inverse transform of (2-3), which reads

$$\hat{\sigma}(\omega) = \frac{1}{2\pi} \int_0^{\infty} u^2(x) J_1(\omega x) dx, \quad (2-8)$$

we then obtain a continuous spectrum<sup>4</sup>

$$\hat{\sigma}(\omega) = \frac{1}{2\pi} \sum_k \hat{\sigma}_k \frac{\omega J_0(\omega) J_1(\omega_k)}{\omega_k^2 - \omega^2}. \quad (2-9)$$

However, for handling the observational data more tractable are discrete spectra. For instance, by extending formally (2-6) to the region  $x > 1$ , we get

$$\hat{\sigma}(\omega) = \frac{1}{2\pi} \sum_k \hat{\sigma}_k \frac{\delta(\omega - \omega_k)}{\omega}. \quad (2-10)$$

Now, the corresponding  $u^2(x)$ , calculated from equation (2-3), can behave quite odd for  $x > 1$  and become even negative! Nevertheless, both (2-9) and (2-10), when substituted to (2-3), lead to the same  $u^2(x)$  for any  $x \in (0, 1)$ . Although the corresponding surface mass densities differ from each other also for  $\rho < R$ , the difference is, in practice, negligible close to the centre. We may therefore accept (2-10) as a first approximation of  $\hat{\sigma}(\omega)$ . By substituting (2-10) to (2-1) we obtain

$$\sigma(\rho) = \frac{v_R^2}{GR} \frac{1}{2\pi} \sum_k \hat{\sigma}_k J_0\left(\omega_k \frac{\rho}{R}\right), \quad \rho \ll R. \quad (2-11)$$

Despite that close to  $R$  equation (2-11) is not a trustworthy approximation (the sum may become negative), it almost perfectly agrees (usually for  $\rho < 0.6R$ ) with the surface densities corresponding to several model rotation curves that were cutting-off at different  $R$ .

## 2.3. The iteration scheme

From the above, it is evident that the total mass of the galactic disk within the cutoff radius cannot be determined from its rotation law only. However, if additional bounds for the surface mass density are known outside the cutoff radius, one may find a reliable global mass distribution by iterations.

As before we denote by  $R$  the cutoff radius, to which a rotation curve has been measured. We denote this part of rotation curve by  $v_0$ . The distribution of matter, which extends far beyond the cutoff radius and which is mostly composed of neutral and molecular hydrogen, we denote by  $\sigma_H$ . If such data are not available, one may try to devise a physically plausible profile of baryonic matter outside  $R$ .

<sup>2</sup>Equation (2-5) is deliberately presented in the form containing only squares of rotational velocity. Much more familiar is its equivalent form given in the Binney & Tremaine [1987] handbook, and therefore commonly used, however it has the deficiency of containing derivatives of  $v^2(\rho)$  which are determined experimentally with very low accuracy.

<sup>3</sup> however, the relation serves as a consistency check of our final results we obtain iteratively later on

<sup>4</sup>Since  $J_0(\omega) \approx J_1(\omega_k)(\omega_k - \omega)$  when  $\omega \approx \omega_k$ , the components under the summation sign are continuous functions of  $\omega$

At the very beginning we define  $u(x) \equiv v_0(Rx)/v_0(R)$ . We calculate from (2-11) an initial surface density  $\sigma_0$  where the corresponding spectral coefficients  $\hat{\sigma}_k^{(0)}$  are calculated from (2-7) (we put  $\sigma_0$  and  $\hat{\sigma}_k^{(0)}$  in place of  $\sigma$  and  $\hat{\sigma}_k$ , respectively). Let  $R_1$  be the first value of  $\rho$  where  $\sigma_0(\rho) = \sigma_H(\rho)$ . The first approximation  $\sigma_1$  to the sought global surface density for  $\rho < R_1$  is defined by setting  $\sigma_1 = \sigma_H$ , and for  $\rho > R_1$  we set  $\sigma_1 = \sigma_0$ . With this  $\sigma_1$  we begin the first iteration step ( $i = 1$ ) which is described below for arbitrary  $i$ .

**The  $i^{\text{th}}$  iteration step** By setting  $\sigma = \sigma_i$  in equation (2-4) we calculate the corresponding approximation  $v = v_i$  to a global rotational velocity. Afterwards we find the resulting discrepancy function  $\delta v_i^2 = v_0^2 - v_i^2$  defined for  $\rho < R$ . The function measures an approximation error in the  $i^{\text{th}}$  iteration step and is used also to determine a correction  $\delta\sigma_i$  to the actual global surface mass density  $\sigma_i$ . By substituting  $\delta v_i^2(xR)/\delta v_i^2(R)$  in place of  $u^2(x)$  in equation (2-7) we find spectral coefficients  $\delta\hat{\sigma}_k^{(i)}$  where now  $\hat{\sigma}_k$  stands for  $\delta\hat{\sigma}_k^{(i)}$ . Next we calculate for  $\rho < R$  the correction  $\delta\sigma_i$  from equation

$$\delta\sigma_i(\rho) = \frac{\delta v_i^2(R)}{2\pi GR} \sum_k \delta\hat{\sigma}_k^{(i)} J_0\left(\omega_k \frac{\rho}{R}\right),$$

which is analogous to equation (2-11). Let  $R_{i+1}$  be the first value of  $\rho$  where  $\sigma_i(\rho) + \delta\sigma_i(\rho) = \sigma_H(\rho)$ . The corrected global surface mass density  $\sigma_{i+1}$  is found by setting  $\sigma_{i+1} = \sigma_i + \delta\sigma_i$  for  $\rho < R_{i+1}$  and  $\sigma_{i+1} = \sigma_H$  for  $\rho > R_{i+1}$ .

Now the  $i + 1$  iteration step follows. We repeat this procedure until  $\max(\delta v_n^2)$  in the  $n^{\text{th}}$  iteration becomes acceptably small.

### 3. Application of the iteration method to the spiral galaxy NGC 4736

As an example we choose the spiral galaxy NGC 4736. Its rotation curve excludes the massive spherical halo, therefore the global disk model should better approximate the gravitational field in this galaxy than models assuming such a halo.

There is also the additional information about distribution of hydrogen observed in the remote region of this galaxy, where the rotation curve has not been determined. This provides the lower bound for the surface density. No other luminous matter has been observed there. The amount of hydrogen in this region is comparably small. Its presence allows us to reconstruct the global mass density and predict the rotation curve beyond the presently measured range.

#### 3.1. Observational data

A high resolution rotation curve of the galaxy was adopted from [Sofue et al. 1999]. It was measured out to  $7'$  which corresponds to cutoff radius  $R = 10.38$  kpc (the distance of the galaxy is  $D = 5.1$  Mpc and inclination angle  $i = 35^\circ$  as in [Sofue et al. 1999]). The rotational velocity has been measured with the maximum error

$\delta v = \pm 11$  km/s (attained at  $\rho = 5'$ ) and the average velocity is 168 km/s. Thus the total dynamical mass should be determinable with the accuracy better than  $\approx 10\%$ . We use also the  $50''$  resolution neutral hydrogen surface density published in [Mulder & van Driel 1993] (inclination was corrected from  $40^\circ$  to  $35^\circ$ ), which is consistent with [Bosma et al. 1977]. A  $\beta$ -band surface brightness  $\lambda_\beta$ , where  $\beta = I, V$  or  $B$  is calculated from

$$\lambda_\beta \left[ \frac{L_{\beta,\odot}}{\text{pc}^2} \right] = \frac{\cos(i)}{\tan^2(\text{arcsec})} 10^{0.4(M_{\beta,\odot} - \mu_\beta - 5)}.$$

It is done using the respective luminosity profiles, corrected for galactic extinctions  $\mu_\beta \left[ \frac{\text{mag}}{\text{arcsec}^2} \right]$ , taken from [Munoz-Tunon et al. 1989]. The reference absolute magnitudes for the Sun are:  $M_{I,\odot} = 4.19$  [van den Bosch et al. 2006],  $M_{V,\odot} = 4.83$  [Takamiya & Sofue 2000] and  $M_{B,\odot} = 5.43$  [Carignan 1985].

#### 3.2. Determining the global surface density and the global rotation curve

Below we shall apply the iteration scheme described in section 2.3. We use the same notational conventions as introduced there.

A third order interpolating function  $u^2(x) = v_0^2(Rx)/v_0^2(R)$  ( $v_R \equiv v_0(R) = 125.6$  km/s) is used to find the spectral coefficients  $\hat{\sigma}_k^{(0)}$ . The  $\mu_k$  coefficients in (2-7) fall off quickly to zero, eg.  $\mu_1/\mu_{125} \approx 3 \times 10^{-6}$ , and the functional sequence of partial sums in (2-11) converges quickly. The summation can thus be terminated at some finite  $k$  (we put  $k = 144$ ). This truncated sum is taken as the surface mass density  $\sigma_0(\rho)$ . Next, we set  $\sigma_1(\rho) = \sigma_0(\rho)$  for  $\rho < R_1$ ,  $\sigma_1(\rho) = \sigma_H(\rho)$  for  $R_1 < \rho < R_H$  and  $\sigma_1(\rho) = 0$  elsewhere, where  $\sigma_H(\rho)$  is the azimuthally averaged neutral hydrogen surface density,  $R_1$  was defined in sec. 2.3 and  $R_H = 16.06$  kpc  $> R$ , cf. line ' $\sigma_1$ ' in figure 2. The integrated mass of  $\sigma_1(\rho)$  is

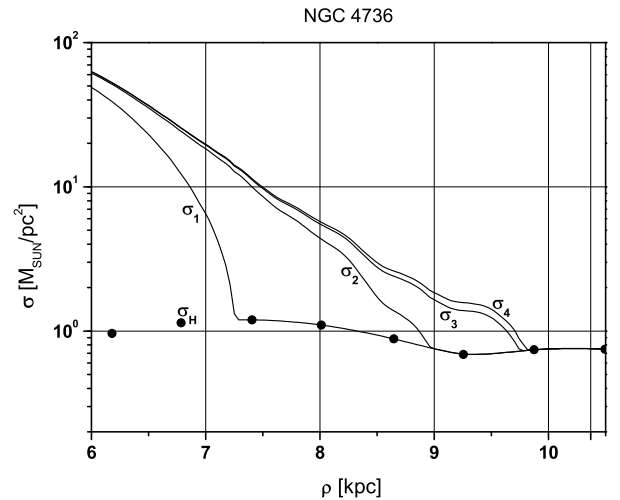


Fig. 2.— A fragment of surface mass density of galaxy NGC 4736 obtained in consecutive iterations (solid lines  $\sigma_1, \sigma_2, \sigma_3, \sigma_4$ ) and the observed column mass density of HI ( $\sigma_H$  – solid circles).

$M_1 \approx 3.144 \times 10^{10} M_\odot$  and should not exceed the total

mass  $M_{TOT}$  more than  $0 < M_{TOT} - M_1 < \delta M_1$ , where  $\delta M_1 < 2Rv_0(R)\text{Max}|v_0 - v_1|/G \approx 5 \times 10^9 M_\odot \approx 0.16M_1$ . The corresponding first approximation  $v_1(\rho)$  to the global rotation curve agrees with  $v_0(\rho)$  very well for the small radii, where  $\sigma_1(\rho)$  is reliable. However, there is still a discrepancy at greater radii, cf. line  $v_1$  in figure 3. In order to reduce it, we find a correction  $\delta\sigma_1(\rho)$  to  $\sigma_1(\rho)$  in the region  $0 < \rho < R$ . The needed spectral coefficients  $\hat{\sigma}_k^{(1)}$  were determined by finding a least square fit to a first order interpolation of  $\delta v_1^2(\rho)$ , with  $xJ_1(\omega_k x)$  used as basis functions.<sup>5</sup> Having found  $\delta\sigma_1(\rho)$  we calculate the corrected surface density in the second approximation  $\sigma_2(\rho) = \sigma_1(\rho) + \delta\sigma_1(\rho)$ , with the reservation we set  $\sigma_2(\rho) = \sigma_H(\rho)$  for  $\rho > R_2$  and  $\sigma_2(\rho) = 0$  for  $\rho > R_H$  (the line ' $v_2$ ' in figure 2). Now, the corresponding global rotation curve  $v_2(\rho)$  agrees with  $v_0(\rho)$  almost perfectly (the line ' $v_2$ ' in figure 3), but it still needs to be corrected a

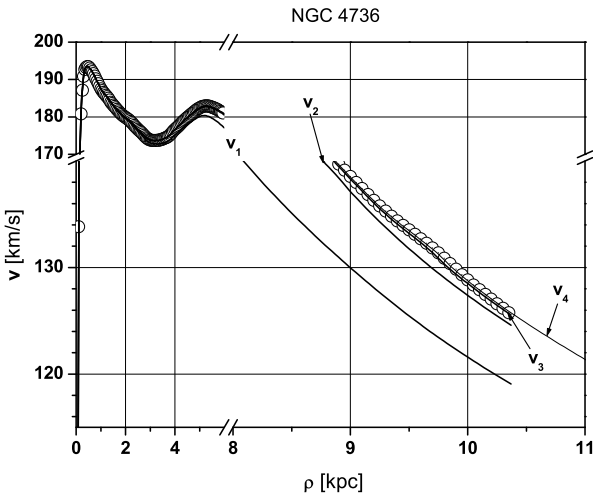


Fig. 3.—  $v_1, v_2, v_3, v_4$  are rotational velocities calculated from equation (2-4) for global surface densities obtained in the four consecutive steps of iteration. The thin line  $v_4$  was shown also outside the observational range (experimental points for NGC 4736 are indicated by circles).

little in the vicinity of,  $R$ , since  $\text{Max}(1 - v_2/v_0) \approx 0.02$ . The corresponding mass is  $M_2 = 3.385 \times 10^{10} M_\odot$  and is underestimated, but  $M_{TOT} - M_2 < \delta M_2$ , where  $\delta M_2 < 2Rv_0(R)\text{Max}|v_0 - v_2|/G \approx 1 \times 10^9 M_\odot \approx 0.03M_2$ . Similarly, we carry out the third step, to find  $\sigma_3(\rho)$  and  $v_3(\rho)$ . The integrated mass in this step is  $M_3 = 3.419 \times 10^{10} M_\odot$  and  $\delta M_3 \approx 3.3 \times 10^8 M_\odot \approx 0.01M_3$ . The error has not changed substantially compared with  $\delta M_2$ , therefore we terminate iterations after the fourth step. In this way we obtain the global surface density  $\sigma_4(\rho)$  shown in figure 4. It gives the total mass  $M_{TOT} = 3.43 \times 10^{10} M_\odot$  (it includes the observed hydrogen HI out to  $R_H$ ), and the corresponding rotation curve  $v_4(\rho)$  – its predicted continuation beyond the cutoff radius can be tested with future observations (see figure 5).

<sup>5</sup>It is known from the theory of generalized Fourier series, that in the theoretical limit of infinite number of terms in the sum (2-6), the values of  $\hat{\sigma}_k$  determined by the least square method would be equal to those calculated from equation (2-7)

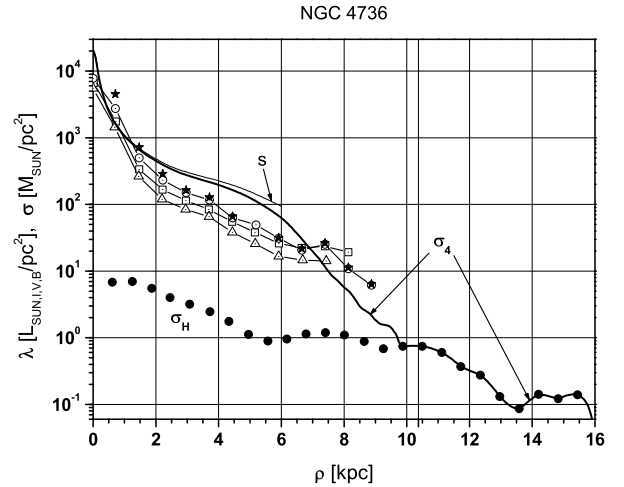


Fig. 4.— Global surface mass density for NGC 4736 found in the fourth iteration (thick solid line  $\sigma_4$ ). This mass distribution leads to rotation velocity that agrees perfectly with the observed rotation curve. For comparison, the surface mass density found in [Takamiya & Sofue 2000] is also shown (the thin line  $s$ ). The observed density profile of hydrogen HI is marked with solid circles. Luminosity profiles  $\lambda(\rho)$  (at inclination angle  $35^\circ$ ) in the  $B$ -band (dotted triangles), the  $V$ -band (dotted squares) and the  $I$ -band (dotted circles) were corrected for galactic extinction [Munoz-Tunon et al. 1989]. The  $I$ -band luminosity was corrected also for the internal extinction (marked with stars).

### 3.3. Discussion

In the previous section we have obtained the surface density in galaxy NGC 4736 that is consistent with distribution of HI beyond the cutoff radius  $R$ , and perfectly agrees with the observed rotation curve. Since HI mass outside  $R$  is only  $0.003M_{TOT}$ , the results (e.g density profile) would not be affected significantly if there was an amount of baryonic matter outside  $R$  comparable to that of HI. The global surface mass density of galaxy NGC 4736 found in the fourth iteration is shown in figure 4 (the ' $\sigma_4$ ' line). The corresponding global rotation curve calculated from equation (2-4) agrees perfectly with the experimental rotation curve  $v_0$ , see figure 5).

The  $V$  and  $B$ -band luminosities are smaller than the  $I$  band luminosity  $L_I$ , cf. table 1 ( $L_V \approx 0.7L_I$  and  $L_B \approx 0.5L_I$ ), which may indicate the presence of dust.

$M_{TOT}$	$3.43 \times 10^{10} M_\odot$
$M_{HI}$	$6.00 \times 10^8 M_\odot \Rightarrow 0.02M_{TOT}$
$L_I$	$2.87 \times 10^{10} L_{I,\odot} \Rightarrow M/L_I = 1.2$
$L_V$	$2.14 \times 10^{10} L_{V,\odot} \Rightarrow M/L_V = 1.6$
$L_B$	$1.54 \times 10^{10} L_{B,\odot} \Rightarrow M/L_B = 2.2$

Table 1: Physical parameters obtained with the help of the Iterative Spectral Method for spiral galaxy NGC 4736. (at the distance  $5.1[\text{Mpc}]$  and inclination angle  $35^\circ$ ).

The mass-to-light ratio profile (surface density to surface luminosity ratio) is shown in figure 6. From the three

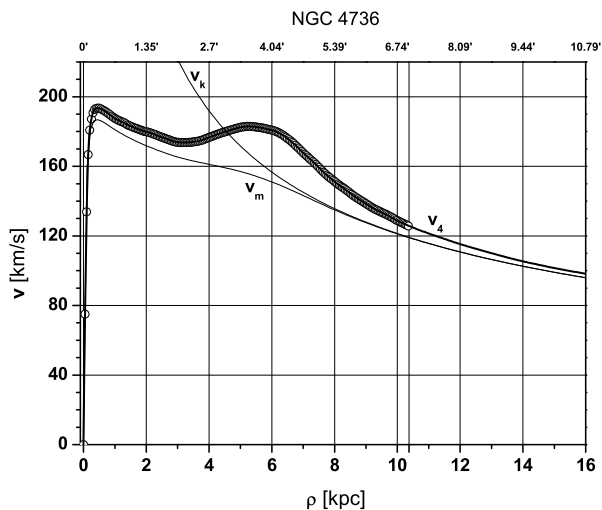


Fig. 5.— The observed rotation curve of galaxy NGC 4736 (circles) and the rotation curve (solid thick line  $v_4$ ) corresponding to surface mass density  $\sigma_4$  found in the fourth iteration and calculated from equation (2-4). The solid thin line  $v_k$  is the corresponding Keplerian asymptote  $\sqrt{GM_{TOT}/\rho}$  where  $M_{TOT} \approx 3.43 \times 10^{10} M_\odot$  is the total galaxy mass. The solid thin line  $v_m$  is the rotational velocity which one would obtain from a spherically symmetric mass distribution with the same mass function as that for NGC 4736.

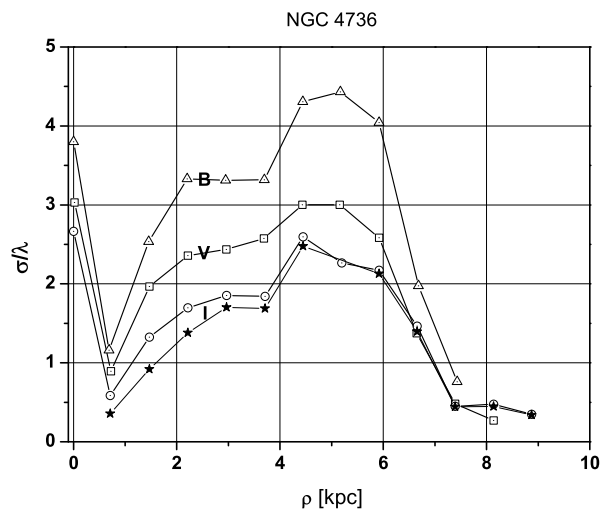


Fig. 6.— The predicted ratios of mass–luminosity surface densities for galaxy NGC 4736 with luminosities corrected for galactic extinction in  $B$ -band (triangles),  $V$ -band (squares),  $I$ -band (circles) and corrected additionally for internal extinction  $I$ -band (marked with stars).

bands, the  $I$ -band should be regarded as the most reliable tracer of the luminous matter, as it most accurately maps the amount of the radiated energy. Luminosity in  $V$ - and  $B$ -bands is reduced by the presence of dust, it also does not include the radiation from low mass stars. For galaxy NGC 4736 the  $I$ -band mass-to-light ratio is

small:  $M/L_I \approx 1.2$ . Also its distribution, i.e. density to luminosity ratio which is of the order of 1 – 2 (cf. figure 6) is typical to stars of slightly sub-solar mass. The total galaxy mass is surprisingly small. It is comparable to the mass predicted in the framework of the MOND model, which gives  $3.21 \pm 0.09 \times 10^{10} M_\odot$ , or in the framework of the metric skew tensor gravity, which gives  $3.15 \pm 0.08 \times 10^{10} M_\odot$  [Brownstein & Moffat 2006]. We obtain  $M_{TOT} = 3.43 \times 10^{10} M_\odot$  for the same rotation curve in the framework of Newtonian physics.

In figure 7 is shown the mass function

$$M_4(\rho)/M_{TOT}, \quad M_4(\rho) = 2\pi \int_0^\rho \sigma_4(\xi) \xi d\xi.$$

It is shown together with the Keplerian mass function  $v_0^2(\rho)\rho/(GM_{TOT})$ , corresponding to the observed rotation curve  $v_0(\rho)$ . The 'odd' behaviour of the latter function was

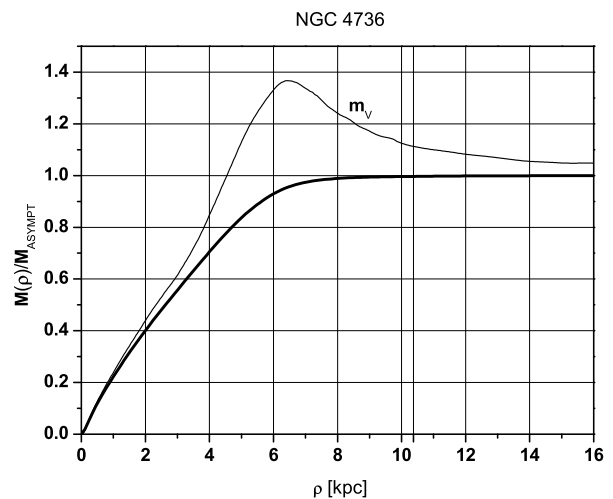


Fig. 7.— Mass function for NGC 4736 normalized with respect to total mass  $M_{TOT} = 3.43 \times 10^{10} M_\odot$  (thick solid line) compared with Keplerian mass function  $m(\rho)$  ( $m_V$  – the thin solid line) defined as  $\rho v_0^2(\rho)/(GM_{TOT})$ , where  $v_0(\rho)$  is the observed rotation curve.

our argument against applying dark halo dominated models to galaxy NGC 4736. Such a model used in [Kent 1987] predicted  $5.0 \times 10^{10} M_\odot$  for the total galaxy mass at a distance 5.1 Mpc. The best fitting curve in that model gives rotational velocity at the cutoff radius 1.2 times greater than the observed value. As this leads to overestimation of the total mass by a factor of some  $(1.2)^2$ , one should expect rather  $5.0 \times 10^{10} M_\odot / (1.2)^2 \approx 3.47 \times 10^{10} M_\odot$  for the total mass, which is very close to our result obtained in the global disk approximation. We note also a related and trivial observation: Keplerian rotation law  $\sqrt{M_4(\rho)G/\rho}$  for a spherically symmetric matter distribution with the mass function numerically equal to  $M_4(\rho)$ , gives smaller rotation velocities at larger radii than the disk model. Also more matter would be required by a spherical model to account for observations, see figure 5.

#### 4. Conclusions

The comparison of mass functions and rotation laws at the end of the previous section, illustrates the fact that the models with flattened mass distributions are more efficient than the commonly used models assuming spherical halo. The former are better in accounting both for high rotational velocities as well as for low scale structure of rotation curves and with noticeably less amount of matter than the latter (the relation between rotation and mass distribution in the disk model is very sensitive for gradients of a rotation curve). The use of the disk model is justified for galaxies with rotation curves violating the sphericity condition. This is necessary (although not sufficient) condition for a spherical mass distribution.<sup>6</sup>

Rotation of the spiral galaxy NGC 4736 can be fully understood in the framework of Newtonian physics. We have found a mass distribution in the galaxy that agrees perfectly with its high-resolution rotation curve, agrees with the *I*-band luminosity distribution giving low mass-to-light ratio of 1.2 in this band at total mass of  $3.43 \times 10^{10} M_{\odot}$ , and is consistent with the amount of HI observed in the remote parts of the galaxy, leaving not much room (if any) for dark matter. Remarkably, we have achieved this consistency without invoking the hypothesis of a massive dark halo nor using modified gravities.

There exist a class of spiral galaxies, similar to NGC 4736, that are not dominated by spherical mass distribution at larger radii. Most importantly, in this region rotation curves should be reconstructed accurately in order not to overestimate the mass distribution. For a given rotation curve it can be easily determined whether or not a spherical halo may be allowed at large radii by examining the Keplerian mass function corresponding to the rotation curve (the so called sphericity test).

By using complementary information of mass distribution, independent of rotation curve, we overcame the cutoff problem for the disk model, that for a given rotation curve, a mass distribution could not be found uniquely as it was dependent on the arbitrary extrapolation of the rotation curve.

One of the authors (MK) was supported by the Polish Ministry of Science and Higher Education, grant 1 P03D 005 28.

#### REFERENCES

- Binney, J., and Tremaine, S. 1987, Galactic dynamics (Princeton Univ. Press)
- Dutton, A. A., van den Bosch, F. C., Dekel, A., and Courteau, S. 2006, preprint (astro-ph/0604553v1)
- Bosma, A., van der Hulst, J. M., and Sullivan III, W. T. 1977, A&A, 57, 373
- Brownstein, J. R., and Moffat, J. W. 2006, ApJ, 636, 721
- Carignan, C. 1985, ApJS, 58, 107

- Kent, S. M. 1987, AJ, 93, 816
- Kostov, V. 2006, preprint (astro-ph/0604395v1)
- Kuijken, K., and Gilmore, G., 1989 MNRAS, 239, 605, 651
- Lebediev N. N., 1953, Special functions and their applications (Moscow)
- Massey, R. 2007, Nature, 445, 286
- Mulder, P. S., and van Driel, W., 1993 A&A, 272, 63
- Munoz-Tunon, C., Prieto, M., Beckman, J., and Cepa, J., 1989, Ap&SS156, 3001
- Nordsieck, K. H. 1973, ApJ, 184, 735
- Romanowsky, A. J. 2003, Science, 301, 1696
- Ryzhik, I. M., and Gradshteyn, I. S. 1951, Tables of Integrals, sums, series and products (Moscow, Leningrad)
- Sofue, Y., and Rubin, V. 2001 ARA&A39, 137
- Sofue, Y., Tutui, Y., Honma, M., Tomita, A., Takamiya, T., Koda, J., and Takeda, Y. 1999, ApJ, 523, 136.
- Takamiya, T., and Sofue, Y. 2000, ApJ, 534, 670
- Toomre, A. 1963, ApJ, 138, 385

<sup>6</sup>A thin disk with surface density  $\sigma(x) = (1 + x^2)^{-3/2} / (2\pi)$  rotates with velocity  $v(x) = x(1 + x^2)^{-3/4}$ . This rotation law satisfies the sphericity condition:  $(xv^2(x))' = 3x^2(1 + x^2)^{-5/2} > 0$ .